

A Comparative Study of Cryorolling and Cryo-Cross Rolling Treatment on Tensile and Fracture Properties of Al 5052 Alloy



Ruby Pant, Amit Joshi, Shushant Singh, Manoj Kumar Pathak, and Saurabh Gairola

Abstract In present study, Al 5052 alloy was cross rolled at cryogenic temperature up to a true strain of 2.3. The impact on microstructure, mechanical, and fracture behaviour is then examined. The microstructure is characterised through optical microscopy and TEM, which shows the formation of ultrafine-grained (UFG) structure in cryo-cross rolled (CCR) samples. Reduction in grain size of CCR samples leads to improvement in tensile properties as a direct consequence of the Hall–Petch effect. As the UFG structure is formed, CCR samples demonstrate a simultaneous increment in tensile strength and fracture toughness compared to solution treated (ST) samples and high dislocation density formed during cryo-cross rolling. The conventional rolling at a cryogenic temperature known as cryorolling (CR) was also performed on Al 5052, and the results were compared with CCR. CCR samples revealed higher ductility enhancement from 7.38% to 10.64% for all sample conditions with respect to CR samples because of the change in strain path and recrystallized microstructure. Due to higher dislocation density, the CCR sample indicates higher hardness from 112 to 128HV as compared to CR sample.

Keywords Cryo-cross rolling · Tensile strength · Fracture toughness

R. Pant · S. Singh

Department of Mechanical Engineering, Uttarakhand University, Dehradun, Uttarakhand 248001, India

A. Joshi (✉) · M. K. Pathak

Department of Mechanical Engineering, G. B. Pant Institute of Engineering and Technology, Pauri 246194, India
e-mail: amitiitrebsd@gmail.com

S. Gairola

Department of Engineering Design, Indian Institute of Technology, Madras, Chennai 600036, India

1 Introduction

Aluminium 5052 is a non-heat treatable aluminium alloy based on magnesium [1]. Due to its combined properties like good strength-to-weight ratio, easy to weld, and high corrosion resistance, aluminium 5052 is used in armour plates, and naval plates [1]. Aluminium 5052 is widely accepted as a replacement for conventional Al 5083 alloy in armour plates. It is a good choice for applications in the marine sector due to its excellent strength and corrosion resistance. [2]. Bergquist et al. [3] compared the static and dynamic response of three aluminium alloys (Al 5059, Al 5083, Al 7039) which are potential candidates for armour plates, and he reported the highest tensile strength in Al 7039, but Al 5059 shows the best combination of strength and corrosion resistance. Izadi et al. [4] have investigated grain development patterns and Hall–Petch strength in Al 5059 samples processed by friction stir welding (FSW) and reported the formation of fine-grained structure in FSW samples. Due to its use in armour plating and ships, a lot of research has been dedicated towards ballistic performance [5] and weld joints [4, 5] of aluminium 5059 alloy, but efforts for improving the mechanical properties are scarce in literature.

The strength of non-heat treated alloys can be improved by using strain hardening and solid solution strengthening [6]. Aluminium 5052 alloy derives its superior tensile strength from high magnesium concentration [7]. Although magnesium is soluble in aluminium, a large amount of magnesium in the alloy causes lower ductility and low corrosion resistance [6, 7]. As a result, strain hardening emerges as the most viable option for enhancing the mechanical characteristics of Al 5052 alloy. A wide range of severe plastic deformation (SPD) processes, such as multi-axial forging (MAF) [8, 9], accumulative roll bonding (ARB) [10], and cryorolling (CR) [11–13], have been developed in recent decades for improving the mechanical properties of metals/alloys. SPD process induces high dislocation density which leads to the formation of UFG structure and thereby improves the mechanical properties [14]. Cryorolling is a relatively simple and inexpensive SPD technique that is used to produce UFG structure in various Al alloys [15, 16] and it has the additional benefit of producing output in sheet form as required in the armour plates. Rangaraju et al. [17] have reported the formation of UFG structure in cryorolled commercially pure aluminium which leads to an increase of 134% in tensile strength. Nikhil et al. [15] have reported an increase of 71.17% in the ultimate tensile strength of Al 5052 alloy accompanied by a simultaneous 600% decrease in ductility. Similar results have been observed in Al 6063 alloy by Panigrahi et al. [18]. An increase of 123% in ultimate tensile strength and a decrease of 600% in ductility is observed after cryorolling. These studies show the increase in mechanical properties like tensile strength, and hardness comes at the expense of ductility. The researcher has demonstrated that the ductility of cryorolled samples can be increased by post-rolled annealing or ageing treatment [14, 16]. Annealing improves the ductility of samples by recrystallization and improves the grain size, but as a direct consequence of this increase in grain size, the tensile strength of samples decreases in annealed samples. Despite cryorolling and post-rolled annealing, a new method known as cryo-cross rolling (CCR) has

emerged for enhancing the strength and ductility of metals/alloys at the same time. The CCR method combines the benefits of cross rolling with cryorolling to give deformed materials the best mechanical qualities under a variety of situations.

Despite the potential of improving mechanical properties by UFG formation in Al 5052 alloy, the literature on SPD processing of Al 5052 alloy by use of the CCR method is really scarce. The present work is focused on improving the mechanical and fracture behaviour of Al 5052 alloy by CCR treatment and correlating the changes in mechanical properties and fracture behaviour with microstructural features. Microstructure in the present study is studied using optical microscopy, and tunnelling electron microscopy (TEM) was used to characterise, the tensile and fracture behaviour after CR and CCR treatment is analysed through the tensile test and three-point bend test, respectively.

2 Materials

For present study, aluminium 5052 was procured in the form of 40 mm thick sheets in T6 temper condition from BAM, Maharashtra, India. The chemical composition of aluminium 5052 alloys is given in Table 1. The samples of 40 mm (length) * 30 mm (width) * 10 mm (thickness) were cut from 170 mm (length) * 110 mm (width) * 40 mm (thickness) plates. After that, the samples were solution treated for 2 h at 540 °C before being quenched in room temperature water.

These samples were immersed in liquid N₂ for fifteen minutes before going through the rollers, then dipped again for 10 min before each pass until an effective true strain of 2.3 was achieved. Researchers have utilised a similar cryorolling process to create the UFG structure [19]. The microstructure of cryorolled and cross rolled samples was observed through optical microscopy and tunnelling electron microscopy (TEM). Optical microscopy samples were polished using varied grit emery paper sizes up to 2000, followed by cloth polishing using a polishing cloth and an abrasive slurry of MgO. These samples were then etched through Poultons reagent and observed under Leica DMI 5000 using polarised light. As for analysis by TEM, samples were prepared through mechanical grinding using emery paper of various grit size ranging from 250 to 1200 followed by polishing through ion beam milling. At 120 V, TEM was performed on a Philips CM 12 microscope. Various tests, including as tensile tests, hardness tests, and 3-point bend test, are used to find out the mechanical and fracture behaviour of CR and CCR samples. Tensile test samples were manufactured and analysed according to the ASTM E8 sub-size standard on H25K-S Tinius Oslen using a strain rate of $5 * 10^{-4}$. Detailed specifications

Table 1 Composition of aluminium 5052 alloy

Element	Si	Fe	Cu	Mn	Mg	Cr	Zn	Al
Composition (wt. %)	0.21	0.37	0.11	0.09	2.34	0.29	0.11	Balance

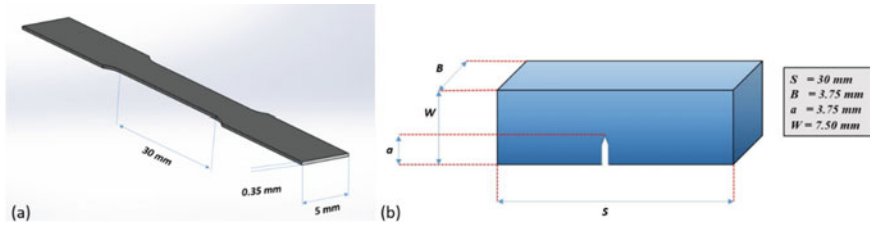


Fig. 1 Specification of: **a** tensile sample and **b** three-point bend sample

of tensile samples are shown in Fig. 1a. Vickers hardness testing rig was used to measure the hardness of samples by using a five kilogram-force load for a dwell time of fifteen seconds. Hardness is measured in different locations in individual samples, and an average of five readings is taken as a final result. Three-point bend samples were prepared as per American Society for Testing and Materials (ASTM) standard, and the test was performed on H25K-S Tinius Oslen using the special attachment. Specification of 3-point test specimens is shown in Fig. 1b. Field emission scanning electron microscopy (FESEM) study shows the fracture surface after tensile and 3-point bend tests.

3 Experimental Procedure

3.1 Microstructure Characterisation

3.1.1 Optical Microscopy

After solution treatment and cryorolling, the microstructure of aluminium 5052 is characterised through optical microscopy and TEM analysis. Figure 2 shows the optical microscopy of samples in different processing conditions. Solution treatment of Al 5052 alloy led to the formation of a uniformly distributed equi-axed structure with an average grain size of 200 μm , as seen in Fig. 2a.

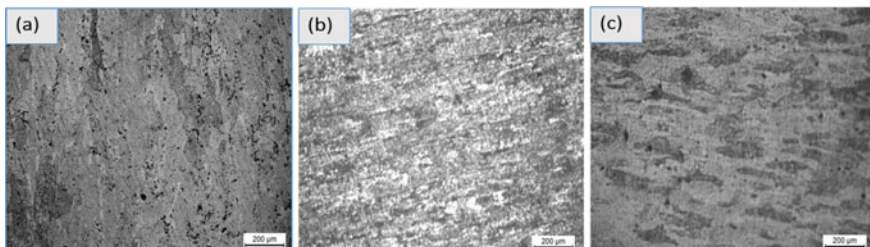


Fig. 2 Optical microscopy in diverse processing conditions: **a** ST, **b** CR 90%, and **c** CCR 90%.

After CR up to 90% thickness reduction, grains become elongated in the rolling direction, as seen in Fig. 2b. Cryorolling leads to the deformation of well-defined grain boundaries formed during solution treatment and converts them into ill-defined deformation cells as described by many researchers [6, 14], but due to the limited magnification of optical microscopy, we need TEM to observe the formation of UFG structure after cryorolling. The optical microstructure of CCR samples with 90% thickness reduction is shown in Fig. 2c. CCR samples showed ill-defined grain boundaries. However, the thickness of the grains is slightly more as compared with CR 90% samples. This may be due to the cross rolling effect resulting wider grain structure as observed in Fig. 2b.

3.2 Tunnelling Electron Microscopy (TEM), and Electron Back-Scattered Diffraction (EBSD) Analysis

TEM results of CR 90% samples subjected to the true strain of 2.3 are shown in Fig. 3a. CR samples showed entangled dislocation cells and substructures elongated in rolling direction surrounded by an ill-defined grain boundary. The size of these dislocation substructures is well within the UFG regime, as seen in Fig. 3a. Areas with high dislocation density, which is a characteristic feature of all SPD processes can be seen distributed over the whole surface of CR samples [9]. The microstructure of annealed samples differs significantly from that of cryorolled samples. Figure 3c and d depicts the TEM results of CCR samples subjected to a true strain of 2.3. The density of dislocations has decreased even further in these samples, while the size of the dislocation sub-structure has increased. These samples show a significantly lower dislocation density compared to the CR samples, as shown in Fig. 3d. The size and width of grains increases due to the cross rolling effect, as observed in these figures. The misorientation distribution of the cryorolled and cross-cryorolled samples is depicted in Fig. 3e and f, respectively. Misorientation distribution of both CR and CCR samples shows a very high fraction of low-angle grain boundaries (LAGB, grain boundaries less than 15°). The high fraction of the LAGB can be attributed to the formation of the deformation substructures such as sub-grains in CR and CCR samples.

3.3 Mechanical Behaviour

Figure 4 and Table 2 show the mechanical properties of Al 5052 alloy in different processing conditions. Aluminium 5052 alloy in ST condition has a yield strength of 81 MPa and ultimate tensile strength of 170 MPa. After cryorolling, yield strength and ultimate tensile strength increase to 157.11 MPa and 289 MPa. So, an increase of 94.35% in yield strength and 70.51% in ultimate tensile strength is observed after

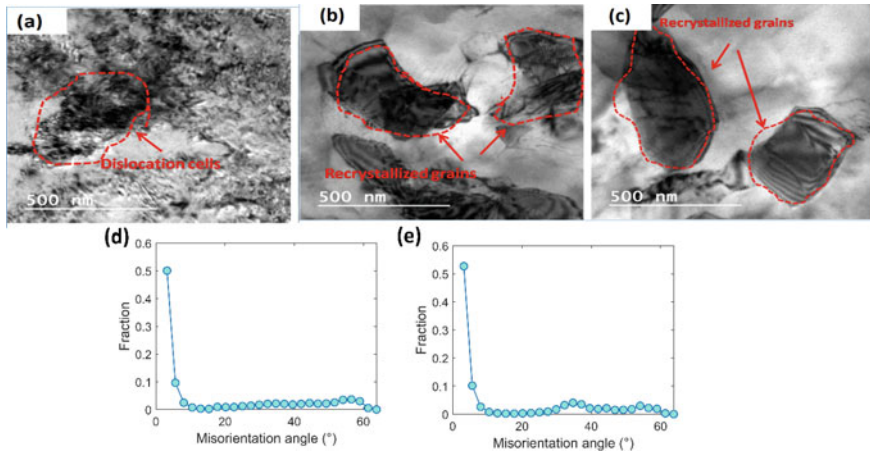


Fig. 3 TEM micrograph for: **a** CR 90%, **b** and **c** CCR 90%. Misorientation distribution of **a** CR 90% and **b** CCR90%

CR treatment. The main reason behind this increase in tensile strength is the fact that CR leads to suppression of dynamic recovery and results in high dislocation density, as confirmed by TEM analysis. The formation of UFG structure after CR treatment also contributes to this increase in tensile strength, as explained by the famous Hall–Petch relationship, but this increase in tensile strength is at the cost of a decrease in ductility. The ductility of Al 5052 alloy decreased by 68.79% (from 23.65% to 7.38%) after CR treatment compared to ST samples. To neutralise these adverse effects of CR treatment, the samples were subjected to cryo-cross rolling (CCR) treatment. Cryo-cross rolled samples show an increment in yield strength (229 MPa) and ultimate tensile strength (436 MPa), and simultaneously an enhancement in ductility (from 7.38% to 10.64%) is also observed in comparison with CR processed samples. Recrystallization and grain enlargement after CCR treatment can be attributable to these changes in mechanical characteristics, as proven by TEM investigation. So, the CCR samples show a significant increase in ductility with simultaneous enhancement in the strength.

The hardness of the aluminium 5052 alloy follows the same trend as seen in the tensile behaviour of different processing conditions. The hardness variation of Al 5052 alloy under different production conditions is shown in Fig. 4c. Cryorolled samples have more hardness as compared with the solution-treated samples. Vickers hardness of solution treated samples comes out to be 52HV, and after cryorolling, it becomes 112HV. The hardness of Al 5052 alloy is increased to 128 HV after CCR treatment. This increase in hardness is due to higher dislocation density and the creation of UFG structure in cryorolled samples. Similar results have been found for different materials subjected to cryorolling [14].

Scanning electron microscopy (SEM) fractography of tensile samples for different processing conditions is shown in Fig. 5. Figure 5a shows the fracture surface of

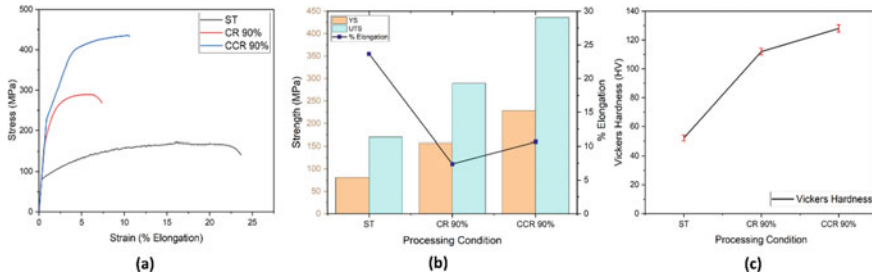


Fig. 4 a Stress–strain curve for ST and CR 90%, CCR 90%. b Variation in tensile properties of Al 5052 for all processing conditions. c Variation of hardness of Al 5052 for all processing conditions

Table 2 Mechanical properties of Al 5052 alloy under the different processing conditions

Processing condition	YS (MPa)	UTS (MPa)	Elongation at fracture (%)	Vickers hardness (HV)	$K\alpha$ (MPa \sqrt{m})
ST	81	170	23.65	52	19.45
CR 90%	157	289	7.38	112	23.32
CCR 90%	229	436	10.64	128	34.41

tensile test specimen of solution treated samples. This increase in hardness is due to higher dislocation density and the creation of UFG structure in cryorolled samples. The dimples in the fracture surfaces of samples subjected to various processing condition are marked by the yellow sphere in Fig. 5. In CR samples, the dimples size is significantly lower compared to the solution treated samples which is a clear indication of the formation of UFG structure in CR samples. In addition to the fine size dimples, fracture surface of CR samples also has some areas with fine facets which is indicated by a yellow rectangle in Fig. 5b. So, mode of fracture in CR samples is mixed mode. Cross rolling improves the grain size of CR samples by recrystallization and this has a direct consequence on dimple size obtained in SEM fractograph of tensile samples. Cross rolling increases grain size and hence the dimple size also increases as seen in Fig. 5c. This increase in grain size of dimples is accompanied by decrease in the density of areas with flat facets. These changes in CCR sample clearly depict the higher tendency of cross rolled samples towards ductile fracture.

3.4 Fracture Behaviour

Fracture toughness of Al 5052 alloy in different reconditioning condition was analysed through single edge notch bending specimen (as shown in Fig. 1) using three-point bend test. Load-extension curve for the different condition is shown in Fig. 6a. Fracture toughness represents the ability of any material to resist fracture in the presence of a crack. Fracture toughness of aluminium 5052 under different processing

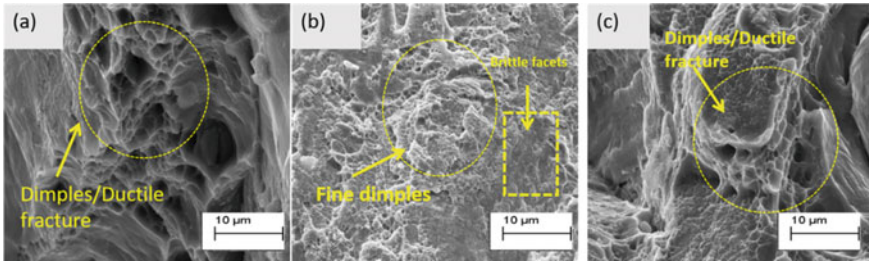


Fig. 5 Fracture surface morphology of Al 5052 alloy after tensile test: **a** ST; **b** CR 90%; and **c** CCR 90%

condition is shown in Fig. 6b. The procedure used in present study for the determining fracture toughness has already been used by various researchers for different alloys [6, 12, 15]. In three-point bend test, high-intensity tri-axial stress is induced in the samples resulting in failure under low loads.

$$B = 2.5 \left(\frac{K_Q}{\sigma_0} \right)^2 \tag{1}$$

B obtained from the above equation must be lower compared to other parameters like crack length (a), specimen thickness (B) and unbroken ligament (b) If this criterion is met, the calculated fracture toughness is known as plane strain fracture toughness; if the samples do not match the criteria, the fracture toughness is known as apparent fracture toughness. K_Q in the above equation is calculated by the following formula:

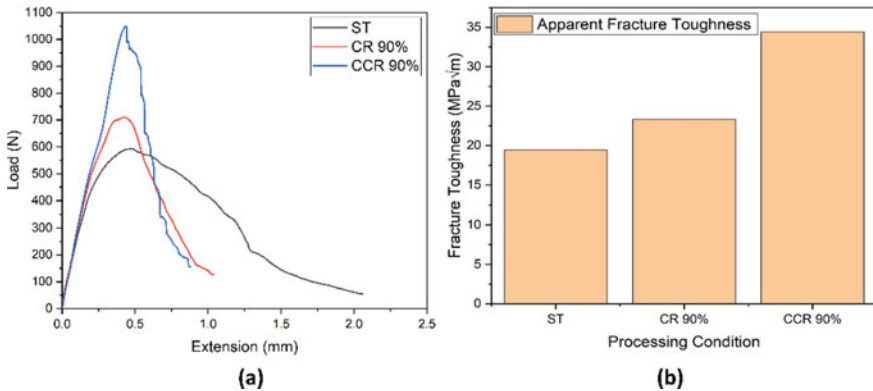


Fig. 6 **a** Comparison of force versus displacement diagram for different processing condition; **b** Comparison of apparent fracture toughness in different processing condition

$$K_Q = \frac{P_Q \cdot S}{B \cdot W^{1.5}} \left[2.9 \left(\frac{a}{w} \right)^{0.5} - 4.6 \left(\frac{a}{w} \right)^{1.5} + 21.8 \left(\frac{a}{w} \right)^{2.5} - 37.6 \left(\frac{a}{w} \right)^{3.5} + 38.7 \left(\frac{a}{w} \right)^{4.5} \right] \quad (2)$$

Substituting the values of KQ in Eq. 2 or solution treated samples comes out to be 19.45 MPa√m. From Eq. 1, the value of B for all sample conditions comes out to be greater than the thickness of specimen and hence samples prepared in the current study fail to satisfy the criteria and hence fracture toughness obtained in the present study is apparent fracture toughness. Apparent fracture toughness for all processing conditions is shown in Fig. 6b.

Fracture toughness of Al 5052 alloy is improved after CR and CCR treatment. This increment might be due to formation of UFG structure and dislocation tangle zones in the CR and CCR samples as shown by TEM results. However, CCR samples showed the higher fracture toughness parameter (apparent fracture toughness) in comparison with CR and ST samples. According to numerous researchers, high dislocation density and dislocation tangles in CR samples promote a delay in fracture onset [20, 21]. The smaller size of grain in CR samples offers increased resistance to the movement of dislocation during loading leading to higher fracture toughness in cryorolled samples as compared to ST samples. CCR treatment further increases the fracture toughness due to the increase in grain size resulting improvement in crack propagation phase. The improved crack propagation phase leads to the enhanced fracture toughness of CCR alloys as compared to CR and ST alloy.

3.5 Fractograph After Three-Point Bend Test

The fracture surface of aluminium 5052 alloy under different processing conditions was characterised by SEM fractography. Figure 7 shows the fracture surface morphology of ST, CR, and CCR samples subjected to a three-point bend test. Solution-treated samples of the fracture surface are shown in Fig. 7a. The fracture surface of solution-treated samples shows a mixture of dimples, brittle facets, and micro-cracks which shows fracture in mixed mode the solution-treated samples. CR sample shows a mixture of flat facets and fine dimples as seen in Fig. 7b which shows the mixed mode of fracture. It might be due to the fact that crack initiation has become easy on account of softening caused by recovery which lowers the fracture toughness values as compared to CCR sample. After CCR, large amount of fine dimples is observed in the fracture surface as seen in Fig. 7c. This indicates that significant amount of plastic deformation has taken place before the failure has occurred in CCR sample resulting significant improvement in resistance to crack initiation and crack propagation phases due to which the fracture toughness of the CCR sample has improved dramatically. It could be related to the establishment of the UFG structure following CCR. A similar observation was made by Joshi et al. [6] during cryorolling and followed by annealing of Al 2014 alloy.

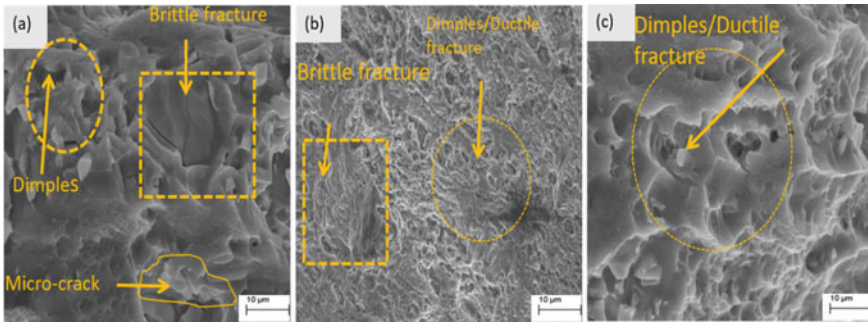


Fig. 7 Fracture surface morphology of Al 5052 alloy after 3 PB test: **a** ST; **b** CR 90%; and **c** CCR 90%

4 Conclusion

The effects of CR and CCR treatment on the aluminium 5052 alloy were explored in this study, and the following results were reached:

- Cryorolled samples have significantly higher tensile strength than ST samples. After cryorolling, YS is increased by 94.34%, while UTS is increased by 70.51%, and this rise in tensile strength is accompanied by a loss in ductility, which has decreased from 23.65% to 7.38 per cent. The formation of UFG structure and high dislocation density is the key factors behind these change in mechanical characteristics.
- The hardness of samples shows a similar trend as tensile strength. The hardness of Al 5052 is increased from 52 to 112 HV after CR, and the value of 128 HV is achieved for CCR-treated samples. This extraordinary improvement in tensile strength and hardness of Al 5052 alloy is attributed to the formation of UFG structure and high dislocation density in cryorolled samples.
- The fracture toughness of samples is also improved after CR and CCR treatment. Apparent fracture toughness value of $34.41 \text{ MPa}\sqrt{m}$ is obtained in CCR-treated samples and $23.32 \text{ MPa}\sqrt{m}$ in CR samples. Reduction in grain size after CR and CCR treatment increases resistance to crack initiation in Al 5052 alloy.

References

1. Yogesha KK, Joshi A, Kumar N, Jayaganthan R (2017) Effect of cryo groove rolling followed by warm rolling (CGW) on the mechanical properties of 5052 Al alloy. *Mater Manuf Process* 32(12):1336–1344
2. Khademian N, Peimaei Y (2020) Lightweight materials (LWM) in transportation especially application of aluminum in light weight automobiles (LWA). In *International conference on interdisciplinary studies in nanotechnology*, pp. 1–22

3. Perez-Bergquist SJ, Rusty Gray III GT, Cerreta EK, Trujillo CP, Perez-Bergquist A (2011) The dynamic and quasi-static mechanical response of three aluminum armor alloys: 5059, 5083 and 7039. *Mater Sci Eng A* 528(29–30):8733–8741
4. Izadi H, Sandstrom R, Gerlich AP (2014) Grain growth behavior and Hall–Petch strengthening in friction stir processed Al 5059. *Metall Mater Trans A* 45(12):5635–5644
5. Showalter DD, Placzankis BE, Burkins MS (2008) Ballistic performance testing of aluminum alloy 5059-H131 and 5059-H136 for armor applications. Army Research Lab Aberdeen Proving Ground MD, 2008
6. Joshi A, Yogesha KK, Kumar N, Jayaganthan R (2016) Influence of annealing on microstructural evolution, precipitation sequence, and fracture toughness of cryorolled Al–Cu–Si alloy. *Metallogr Microstruct Anal* 5(6):540–556
7. Gubicza J, Chinh NQ, Horita Z, Langdon TG (2004) Effect of Mg addition on microstructure and mechanical properties of aluminum. *Mater Sci Eng A* 387:55–59
8. Kapil R, Jayaganthan R, Gairola S, Verma R (2019) Improvement of fracture toughness of ultra fine grained Al–Li 8090 alloy processed through multi axial forging. *Mater Res Express* 6(8):085064
9. Joshi A, Kumar N, Yogesha KK, Jayaganthan R, Nath SK (2016) Mechanical properties and microstructural evolution in Al 2014 alloy processed through multidirectional cryoforging. *J Mater Eng Perfor* 25(7):3031–3045
10. Jamaati R, Naseri M, Toroghinejad MR (2014) Wear behavior of nanostructured Al/Al₂O₃ composite fabricated via accumulative roll bonding (ARB) process. *Mater Des* 59:540–549
11. Gairola S, Joshi A, Gangil B, Rawat P, Verma R (2019) Correlation of tensile properties and fracture toughness with microstructural features for Al–Li 8090 alloy processed by cryorolling and post-rolled annealing. *Trans Indian Inst Met* 72:1743–1755
12. Pathak MK, Joshi A, Mer KKS, Jayaganthan R (2019) Mechanical properties and microstructural evolution of bulk UFG Al 2014 alloy processed through cryorolling and warm rolling. *Acta Metall Sinica (English Letters)* 32(7):845–856
13. Pathak MK, Joshi A, Mer KKS (2019) Evaluating tensile properties and fracture toughness of Al 2014 alloy processed by different rolling methods. *Mater Res Express* 6(10):105012
14. Joshi A, Yogesha KK, Jayaganthan R (2017) Influence of cryorolling and followed by annealing on high cycle fatigue behavior of ultrafine grained Al 2014 alloy. *Mater Charact* 127:253–271
15. Yogesha KK, Kumar N, Joshi A, Jayaganthan R, Nath SK (2016) A Comparative study on tensile and fracture behavior of Al–Mg alloy processed through cryorolling and cryo groove rolling. *Metallogr Microstruct Anal* 5(3):251–263
16. Pathak MK, Joshi A, Mer KKS (2021) Improvement of tensile and fracture toughness properties of Al 2014 alloy processed by different rolling method followed by post-ageing treatment. *Trans Indian Instit Metals* 74(3):679–689
17. Rangaraju N, Raghuram T, Vamsi Krishna B, Prasad Rao K, Venugopal P (2005) Effect of cryo-rolling and annealing on microstructure and properties of commercially pure aluminium. *Mater Sci Eng: A* 398(1–2):246–251
18. Panigrahi SK, Jayaganthan R (2008) A study on the mechanical properties of cryorolled Al–Mg–Si alloy. *Mater Sci Eng: A* 480(1–2):299–305
19. Pathak MK, Joshi A, Mer KKS, Gupta A (2021) Comparative analysis of tensile properties and fracture toughness of Al 2014 alloy processed by warm rolling and cryo-groove rolling. *Mater Today: Proc* 44 (2021): 1841–1847
20. Pant R, Joshi A, Singh S, Raturi A (2023) Influence of cryo-cross rolling and post-rolled annealing on microstructure and high cycle fatigue properties of Al-5052 alloy. *Metall Microstruct Anal* 12(3):505–514. <https://doi.org/10.1007/s13632-023-00961-3>
21. Pant R, Singh S, Joshi A, Joshi K, Saxena KK (2022) Mechanical performance and characteristics evaluation of material through Cryo rolling process: a review. *Mater Today: Proc* 62:3086–3096. <https://doi.org/10.1016/j.matpr.2022.03.245>